EYE-CLIMA
Verifying emissions of climate forcers

Report on the Evaluation of N_2O from satellites

DELIVERABLE 1.6

Author(s): Hartmut Bösch, Michael Hilker, Stefan Noël

Date of submission: 12-02-2026
Version: 1.0
Responsible partner: University of Bremen
Deliverable due date: 31-12-2025
Dissemination level: Public

Call: HORIZON-CL5-2022-D1-02
Topic: Climate Sciences and Responses
Project Type: Research and Innovation Action
Lead Beneficiary: NILU - Norsk Institutt for Luftforskning

This project has received funding from the European Union's Horizon Europe research and innovation programme under grant agreement No 101081395

Document History

Version	Date	Comment	Modifications made by
0.1	03-02-2026	First Draft	Hartmut Bösch, Michael Hilker, Stefan Noël (University of Bremen)
0.2	09-02-2026	Internal review	Rona Thompson (NILU)
0.3	12-02-2026	Final revised version	Hartmut Bösch
1.0	12-02-2026	Submitted to Commission	Rona Thompson (NILU)

This project has received funding from the European Union's Horizon Europe research and innovation programme under grant agreement No 101081395

Summary

Nitrous oxide (N_2O) is one of the three most important anthropogenic greenhouse gases in terms of radiative forcing, alongside methane and carbon dioxide. Our knowledge on global sources of N_2O is mostly based on a global network of in-situ surface networks that are sparse and unevenly distributed limiting the resolution of surface flux inversions to sub-continental scale and with little information on fluxes in the tropics, sub-tropics and Southern Hemisphere.

Satellites can provide globally dense observations of greenhouse gas mixing ratios and satellites exist that can also measure atmospheric N_2O either in the shortwave-infrared or thermal-infrared spectral range. However, variations in atmospheric column measurements related to surface fluxes are very small and thus satellite measurements so far have not been used robustly to infer surface fluxes.

In this report, we evaluate the latest generation of N_2O retrievals from shortwave-infrared measurements by the GOSAT-2 satellite and thermal-infrared measurement by IASI against the CAMS model to assess the consistency between the different datasets. A key aspect of the two satellite datasets is their different vertical sensitivity with IASI measuring the free troposphere and stratosphere while GOSAT-2 measures the total column including the boundary layer. In principle, these different sensitivities could be used to remove the stratospheric column and to extract lower tropospheric N_2O values.

As expected, we observe a clear zonal structure in the satellite datasets and in CAMS data. However, the comparisons between CAMS and the satellite datasets reveals inconsistent results with higher XN_2O values in IASI and lower XN_2O values in GOSAT-2 compared to CAMS. For high latitudes, IASI also shows lower values. For GOSAT-2, the comparisons to CAMS are hampered by the low coverage, especially over land which is due to the strict quality filters that are applied.

In addition, we have (1) evaluated zonal anomalies of XN_2O and of differences between satellites and CAMS to remove large scale differences, (2) compared selected vertical profiles and (3) directly compared IASI and GOSAT-2 XN_2O. The main conclusion is that observed features are more likely retrieval artifacts rather than real atmospheric features. Such artifacts are of the order of a few ppb which impede with any signals from surface emissions.

The main conclusion from this report is that satellite retrievals of XN_2O need to improve before they can be used with confidence to estimate emissions.

This project has received funding from the European Union's Horizon Europe research and innovation programme under grant agreement No 101081395

TABLE OF CONTENTS

This project has received funding from the European Union's Horizon Europe research and innovation programme under grant agreement No 101081395

1. Introduction

Nitrous oxide (N_2O) is one of the three most important anthropogenic greenhouse gases in terms of radiative forcing, alongside methane and carbon dioxide. Similar to methane and carbon dioxide, the atmospheric N_2O mole fraction has significantly increased since pre-industrial times primarily due to anthropogenic activities. The N_2O mole fraction has reached a value of ~340 ppb which is 25% higher than its pre-industrial value. Over the last four decades, N_2O has increased by 10% with the highest observed growth rate in 2021 (Tian et al., 2024). Although natural sources of N_2O outweigh anthropogenic ones, the increase in N_2O is primarily attributed to an increase in anthropogenic emissions from agriculture, fossil fuel usage and other industrial emissions. The only noticeable sink of N_2O is stratospheric photolysis by UV radiation and reaction with $O(^1D)$, which results in a lifetime of N_2O of 116 +/- 9 years (Prather et al., 2015).

Our knowledge on global sources of N_2O is mostly based on a global network of in-situ surface and aircraft measurements from networks such as AGAGE, NOAA, and CSIRO (Prinn et al., 2018, Francey et al., 2003, Dutton et al., 2023). However, these networks are sparse and unevenly distributed with few sites in Africa, South America, and central Asia limiting the resolution of surface flux inversions to sub-continental scale and with limited information on fluxes in the (sub)-tropics and Southern Hemisphere (Tian et al., 2024).

As has been well demonstrated for CO_2 and CH_4, satellites can provide globally dense observations of greenhouse gases, which can provide constraints on regional sources and sinks. Several satellites exist that can also measure atmospheric N_2O either in the shortwave-infrared or thermal-infrared spectral range. However, the expected signals in atmospheric column measurements related to surface fluxes are very small (a few ppb out of 340 ppb) and so satellite data have not been used robustly for surface flux inversions.

The goal of this deliverable is to evaluate the latest generation of N_2O retrievals from shortwave-infrared measurements by the GOSAT-2 satellite and thermal-infrared measurement by IASI against the CAMS model to assess the consistency between the different datasets.

This project has received funding from the European Union's Horizon Europe research and innovation programme under grant agreement No 101081395

2. Datasets

2.1 GOSAT-2 SWIR total columns

The Greenhouse gases Observing Satellite-2 (GOSAT-2) is a Japanese satellite launched in 2018 to monitor carbon dioxide and methane. It is equipped with the Thermal and Near Infrared Sensor of Carbon Observation Fourier-Transform Spectrometer-2 (TANSO-FTS-2) and the Cloud and Aerosol Imager-2 (TANSO-CAI-2). Similar to TANSO-FTS on GOSAT, the TANSO-FTS-2 does not measure in a continuous swath along its orbit, but makes single point measurements with a pixel diameter of 9.6 km. The observation interval is 4.024 sec, with a nominal turn-around time of 0.65 sec. TANSO-FTS-2 measures in the SWIR and thermal infrared (TIR) regions of the electromagnetic spectrum with a spectral resolution of 0.2 cm^{-1}. It can operate in nadir viewing geometry, but also has a mode to observe sunglint over the oceans, which can be used to provide better measurement quality over the usually dark ocean surface. To reduce cloud-contaminated observations, the line of sight is adjusted during the FTS turn around motion to actively avoid cloudy pixels. Further information about GOSAT-2 can be found in Suto et al. (2021).

For the retrieval of atmospheric trace gases from GOSAT-2 radiance a retrieval algorithm is used. Operational data product from GOSAT-2 products are available from the National Institute for Environmental Studies (NIES). In this report, we have used data products that have been generated with the Fast Atmospheric trace gas retrieval (FOCAL) that has been developed at IUP Bremen (Reuter et al., 2017). This algorithm approximates full-physics retrieval methods by using a scattering approximation based on a single scattering layer. The inverse method of FOCAL is based on the optimal estimation principles described in Rodgers (2000).

The retrieval retrieves the column averaged dry-air model fraction of N_2O called XN_2O from a fit to the radiances in the fit window between 4364 and 4449 cm^{-1}. The retrieval scales an a priori N_2O profile that does not depend on geolocation and is based on the tropical reference atmosphere from Anderson et al. (1986), scaled to a column-average value of 330 ppb. More information on the GOSAT-2 retrieval is given in Noel et al. (2022).

2.2 IASI IR profiles

The Infrared Atmospheric Sounding Interferometer (IASI) is an imaging Fourier Transform Spectrometer and is installed on the Meteorological operational (Metop) satellites of the European Organization for Exploitation of Meteorological Satellites (EUMETSAT). The main purpose of IASI is the support of numerical weather prediction, but it also offers the possibility for atmospheric trace gas retrievals due to its high spectral resolution of 0.5 cm^{-1} and high signal- to-noise ratio. IASI operates in nadir viewing geometry and has a swath width of 2200 km with a 48.3° viewing angle containing 120 pixels with a 12 km pixel diameter at nadir. IASI measures in the thermal infrared spectral range between 635 cm^{-1} and 2760 cm^{-1} (3.63 µm - 15. 5 µm). Further information on IASI can be found in Clerbaux et al. (2009).

Here a dataset of the Multi-Species Integration of Column Atmospheric Observations (MUSICA) IASI retrieval from the Karlsruhe Institute of Technology, described in Schneider et al. (2022) has been used. This dataset has been retrieved using the PROFFIT-nadir retrieval algorithm (Schneider and Hase, 2011). PROFFIT- nadir is an optimal estimation algorithm that retrieves vertical profiles of trace gases such as N_2O. The retrieval uses a spectral fit window of 1190 cm^{-1} – 1400 cm^{-1}, producing profiles with up to 29 altitude levels. The a priori profile for N_2O is time- and latitude-dependent, based on simulations from the coupled chemistry climate Community Earth System Model version 1 - Whole Atmosphere Community Climate Model (CESM1-WACCM) (Marsh et al., 2013). The IASI retrieval retrieves a profile of N_2O vmr which we used to compute a XN_2O value according to:

This project has received funding from the European Union's Horizon Europe research and innovation programme under grant agreement No 101081395

$$XN2O = \frac{\sum_i c_i \cdot vmr_i}{\sum_i c_i}$$

where c_i is the dry air column in layer i and vmr_i is the N_2O volume mixing ratio on layer i.

2.3 CAMS

The model dataset from Copernicus Atmospheric Monitoring Service (CAMS) is a product of the PyVAR-N_2O inversion framework described in Thompson et al. (2014). This framework uses an offline version of the Laboratoire de Météorologie Dynamique model version 6 LMDz6 (Hourdinet al., 2006) to simulate atmospheric transport. For the stratospheric losses of N_2O through reactions with O(1D) and photolysis, the model uses pre-calculated fields from simulations of the online version of the LMDz6 model. The observational input for the inversion comes not from satellites but from a total of 113 ground-based sites, ship and aircraft transects made with gas chromatographs equipped with an electron capture detector. The output fields are resolved at 2.5° × 1.25° with 79 vertical layers (or 80 levels) for every 3 hours.

For the comparison of CAMS to IASI, the averaging kernel $\boldsymbol{A}$ and a priori profile $\boldsymbol{x_a}$ of the IASI retrieval has been taken into account according to:

$$\boldsymbol{x} = \boldsymbol{x}_a + \boldsymbol{A}(\boldsymbol{x}_{CAMS} - \boldsymbol{x}_a)$$

For the GOSAT-2 retrieval, no averaging kernel has been available and we assumed that the normalised column averaging kernel is unity and thus the CAMS XN_2O value can be directly compared to the GOSAT-2 value.

This project has received funding from the European Union's Horizon Europe research and innovation programme under grant agreement No 101081395

3. Comparison between GOSAT-2, IASI and CAMS

3.1 GOSAT-2 and IASI Data

Examples of monthly maps of cloud-free and quality-filtered XN_2O data from GOSAT-2 and IASI XN_2O are given in Figure 1 and Figure 2.

The GOSAT-2 data shows poor coverage for all 4 given months with data being primarily available over the oceans with low coverage over land masses, in particular over northern hemispheric land. This low coverage is the result of the applied quality filters and it can be expected that adjusted filters in future releases can help to increase coverage.

In contrast, we find complete global coverage on a monthly bases with IASI data including all land and ocean surfaces. This reflects the dense and continuous measurements collected by IASI, the ability of IASI to acquire data over land and ocean and much reduced sensitivity to aerosol scattering. However, a major limitation of the IASI data is its lack of measurement sensitivity to the boundary layer.

Both datasets show a clear zonal structure with high values in the Tropics and low values in high latitudes, especially in high latitude winter. This behaviour is well understood and is caused by changes of the height of the tropopause which separates the troposphere with high N_2O values and the stratosphere where N_2O values are lower due to loss via photolysis and reactions with excited oxygen. Similarly, we can observe lower XN_2O values for mountainous regions where the high surface elevation reduces the tropospheric contribution to the total column.

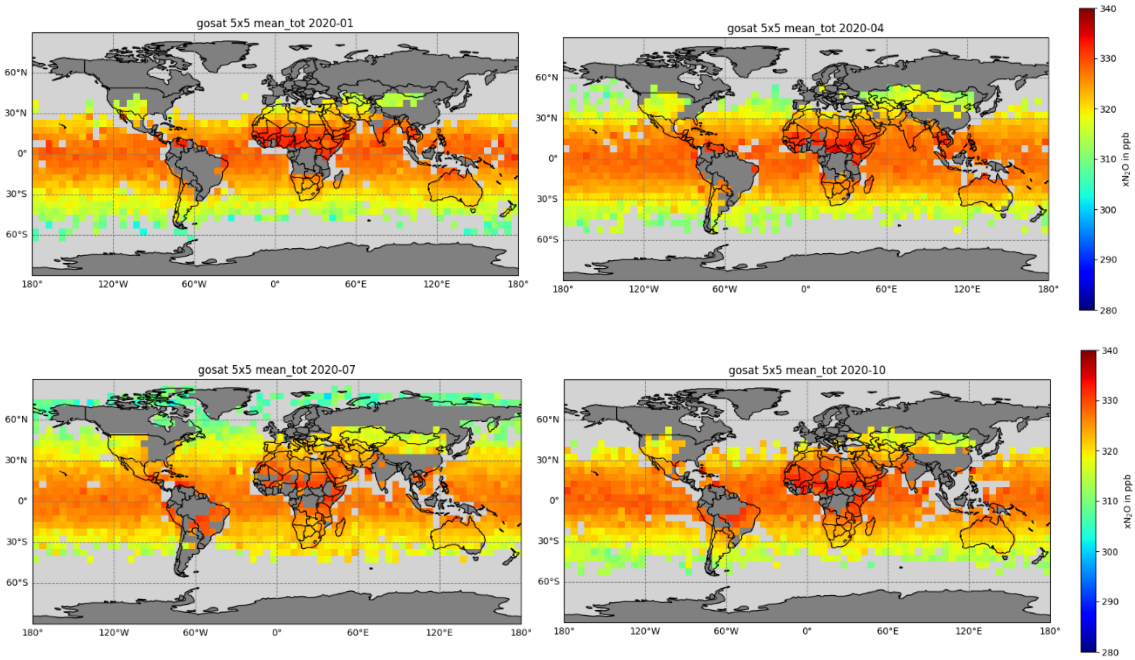

Figure 1: XN_2O from GOSAT-2 for January, April, July and October of 2020 binned into 5° x 5° after cloud and quality filtering

This project has received funding from the European Union's Horizon Europe research and innovation programme under grant agreement No 101081395

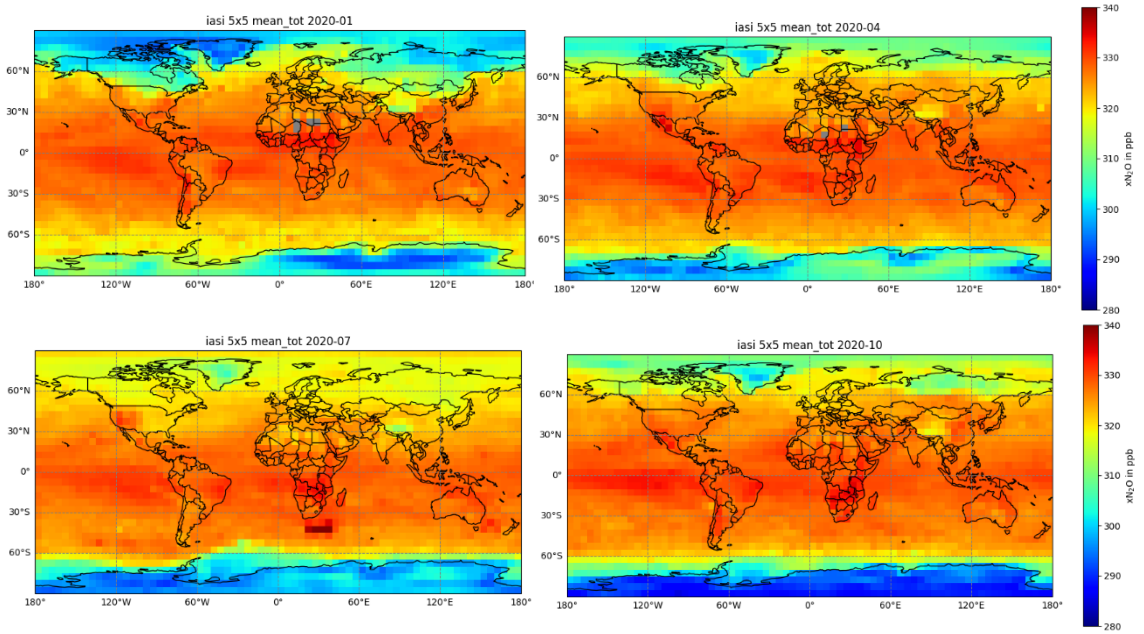

Figure 2: As **Figure 1** but for IASI.

3.2 Comparison between the satellite datasets GOSAT-2 and IASI with CAMS

The gridded XN_2O maps from IASI and GOSAT-2 are shown in Figure 3 and Figure 4 for two months (March and September 2020) together with XN_2O from CAMS. The CAMS data is given with and without the IASI averaging kernel applied, where the maps with averaging kernel should be compared to IASI and without to GOSAT-2. However, application of the averaging kernels results only in minor differences.

The CAMS data shows a similar zonal pattern as is observed in IASI and GOSAT-2. However, as in shown by the difference plots in Figure 5 and Figure 6 (and by the Hovmöller plots in Figure 7 and Figure 8), there are large differences between XN_2O from IASI and CAMS with IASI showing higher values while for high latitudes the opposite is true. For the comparison between GOSAT-2 and CAMS, we find an overestimate by CAMS over the oceans with an underestimate over land. In both cases, the differences between satellites and CAMS are lowest near the equator.

Although these discrepancies may point towards issues in the CAMS model with correct representing stratospheric N_2O loss processes and/or the large-scale Brewer-Dobson circulation, they may also hint at issue with the satellite retrievals. The latter one is supported by the different (and thus inconsistent) signs observed in the differences between CAMS and both satellite datasets and also by the clear land-sea contrast in case of GOSAT-2.

Figure 9 to Figure 11 show vertical N_2O profiles of the CAMS model and the a priori and a posteriori N_2O profile of the IASI retrieval for selected locations and months. Good agreement is seen between the IASI a priori profile and the CAMS profile but with the CAMS model indicating slightly higher values around the Tropopause in Fig. 9 for 35-40°N. The IASI retrieval tends to increase N_2O value in the tropopause region but the most pronounced feature of the IASI retrieval for the two northern hemispheric cases is the large change of the mid-tropospheric values except for November and December for the 50-55°N region. In the southern hemispheric case, we see a larger difference in stratospheric N_2O between the retrieval and CAMS but almost no difference in the troposphere (Fig. 11). This behaviour is unlikely representing real atmospheric N_2O variations and is most likely caused by retrieval shortcomings and by layer-layer correlations in the retrieval causing some oscillating structures.

This project has received funding from the European Union's Horizon Europe research and innovation programme under grant agreement No 101081395

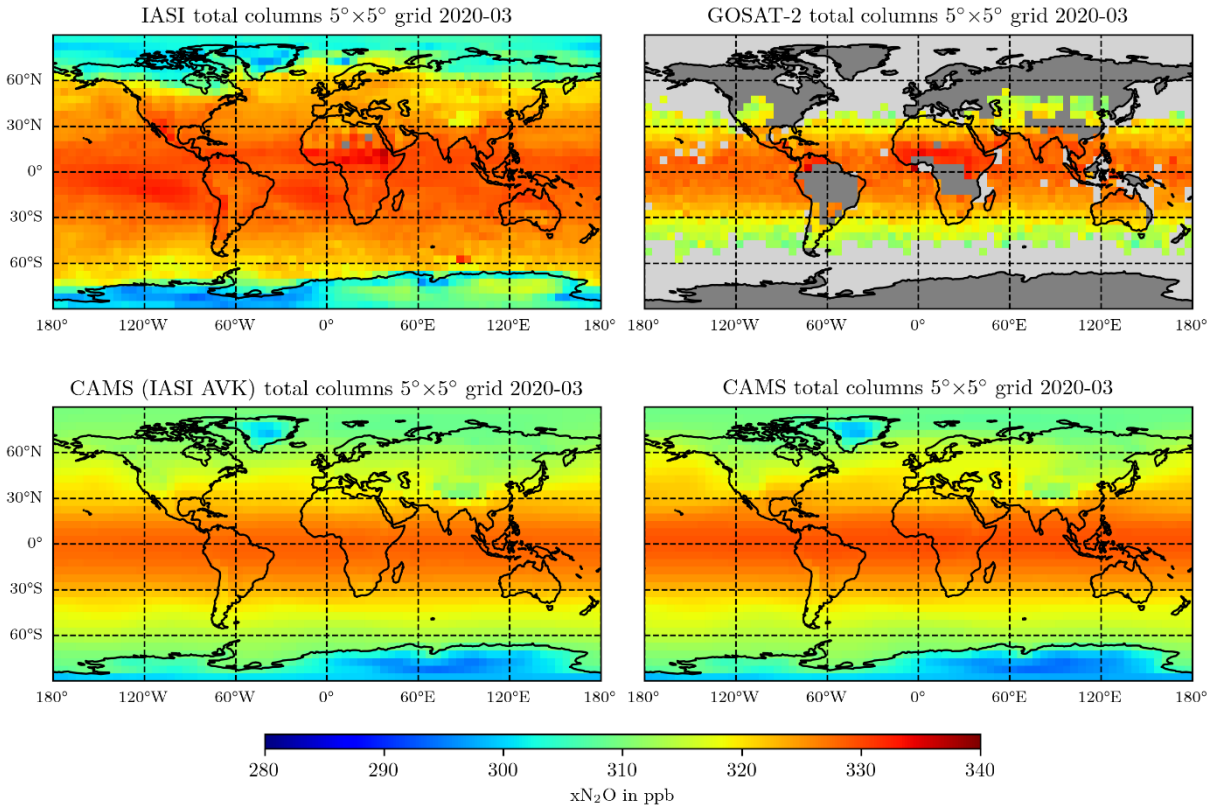

Figure 3: XN2O from IASI (left top), GOSAT-2 (right top), from CAMS (bottom right) and from CAMS with IASI averaging kernels applied (bottom left) for March 2020.

This project has received funding from the European Union's Horizon Europe research and innovation programme under grant agreement No 101081395

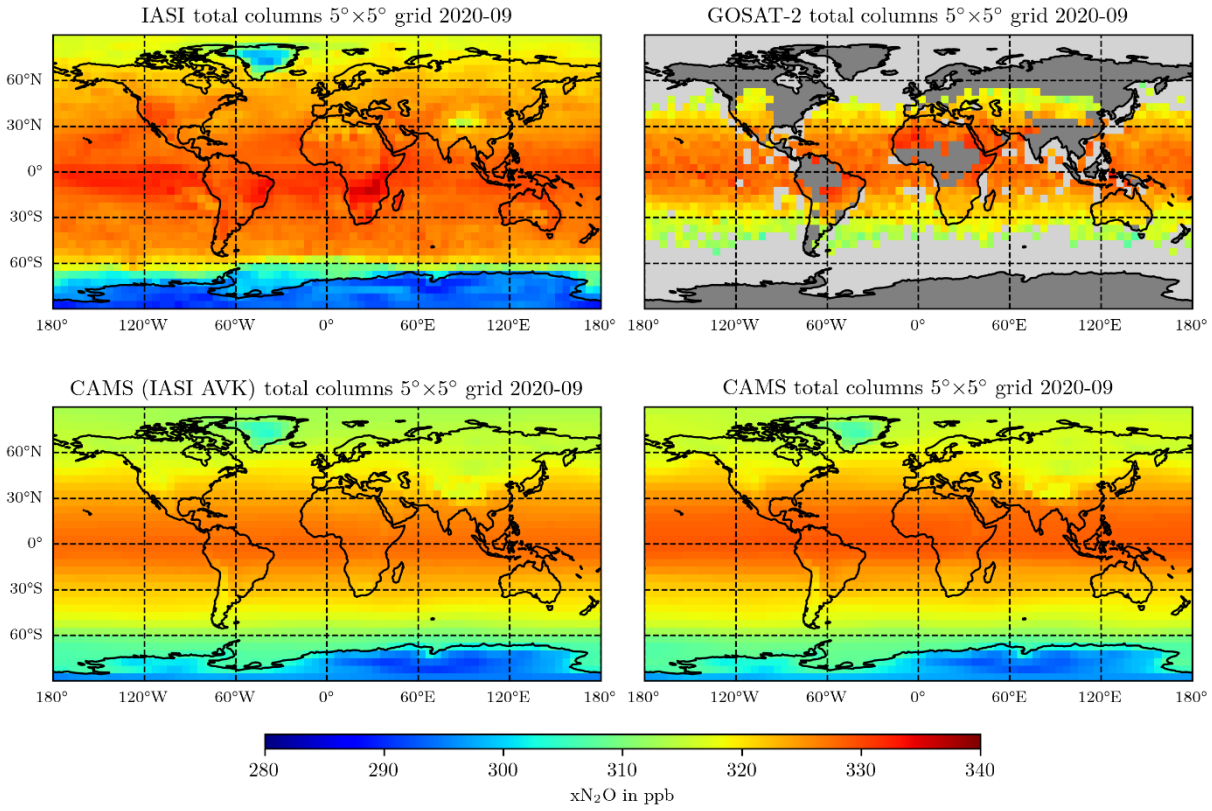

Figure 4: As **Figure 3** but for September 2020

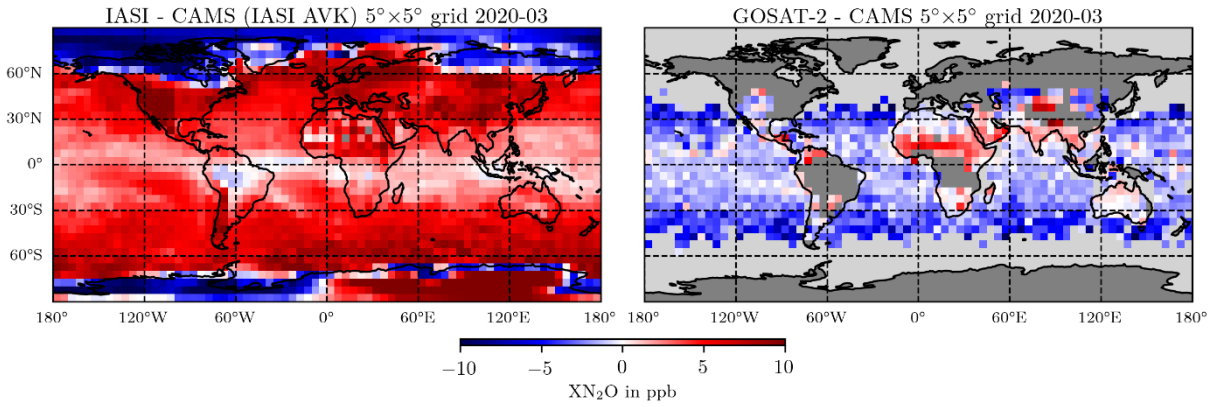

Figure 5: Difference in XN2O between IASI and CAMS (left) and GOSAT-2 and CAMS (right) for March 2020

This project has received funding from the European Union's Horizon Europe research and innovation programme under grant agreement No 101081395

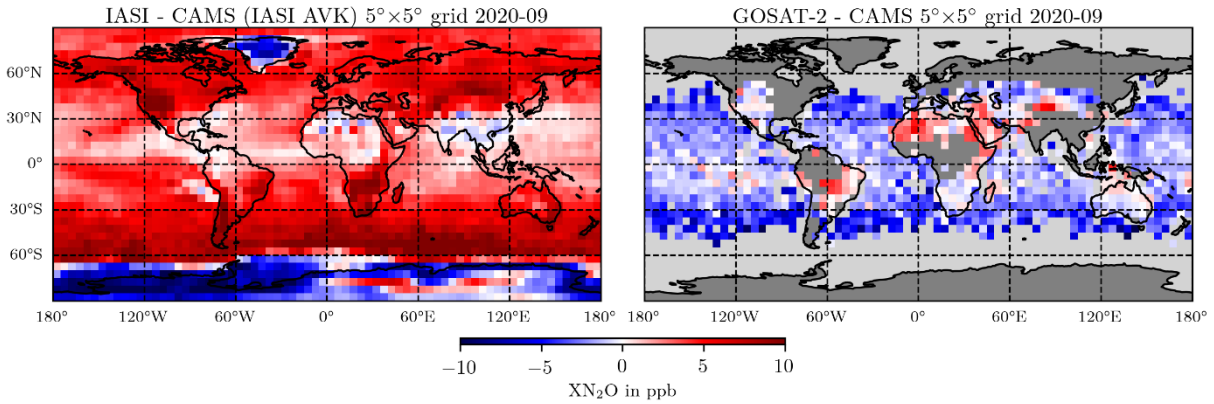

Figure 6: As **Figure 5** but for September 2020.

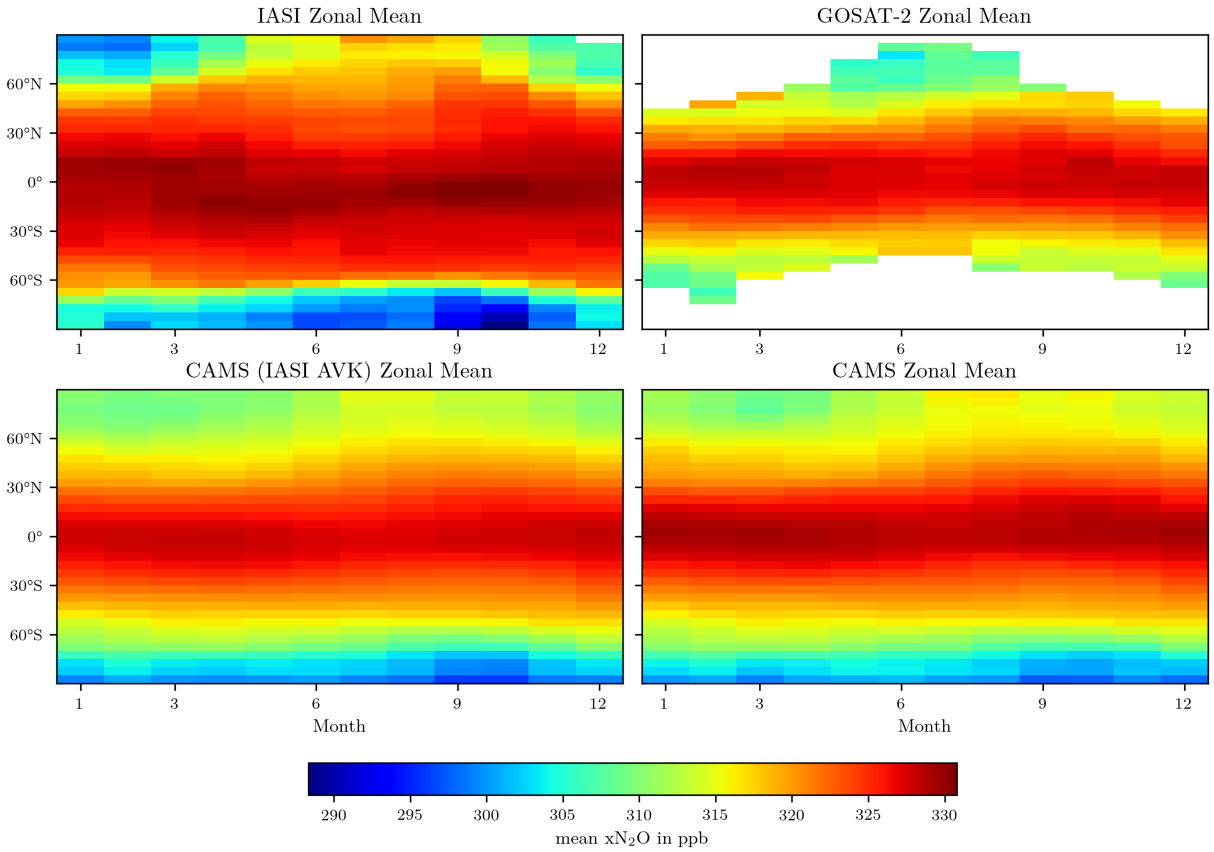

Figure 7: Hovmöller plots of zonally averaged XN2O versus months of the year 2020 for IASI, GOSAT-2, and CAMS with and without IASI averaging kernels applied

This project has received funding from the European Union's Horizon Europe research and innovation programme under grant agreement No 101081395

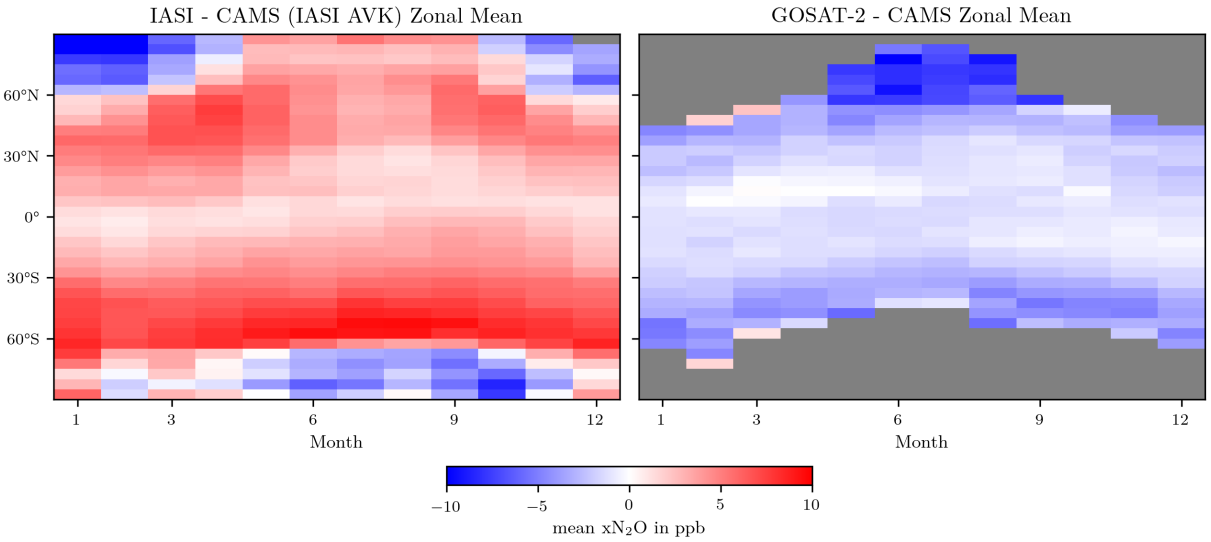

Figure 8: Hovmöller plots of zonally averaged XN2O difference between IASI and CAMS and GOSAT-2 and CAMS

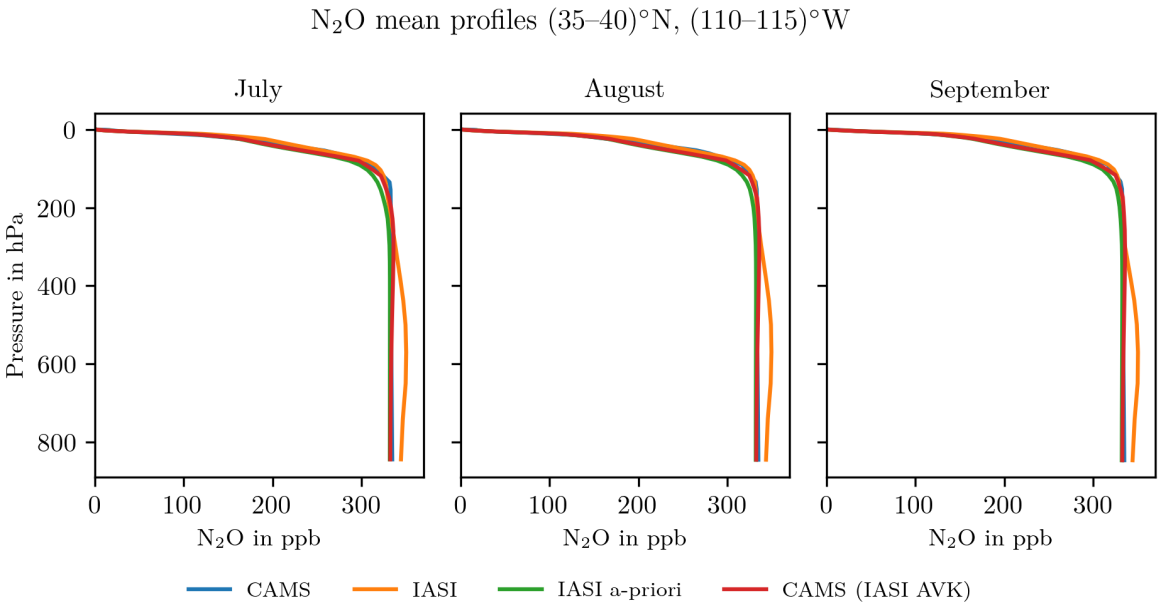

Figure 9: N_2O mean vertical profiles in a grid cell over the Rocky Mountains for July, August and September 2020.

This project has received funding from the European Union's Horizon Europe research and innovation programme under grant agreement No 101081395

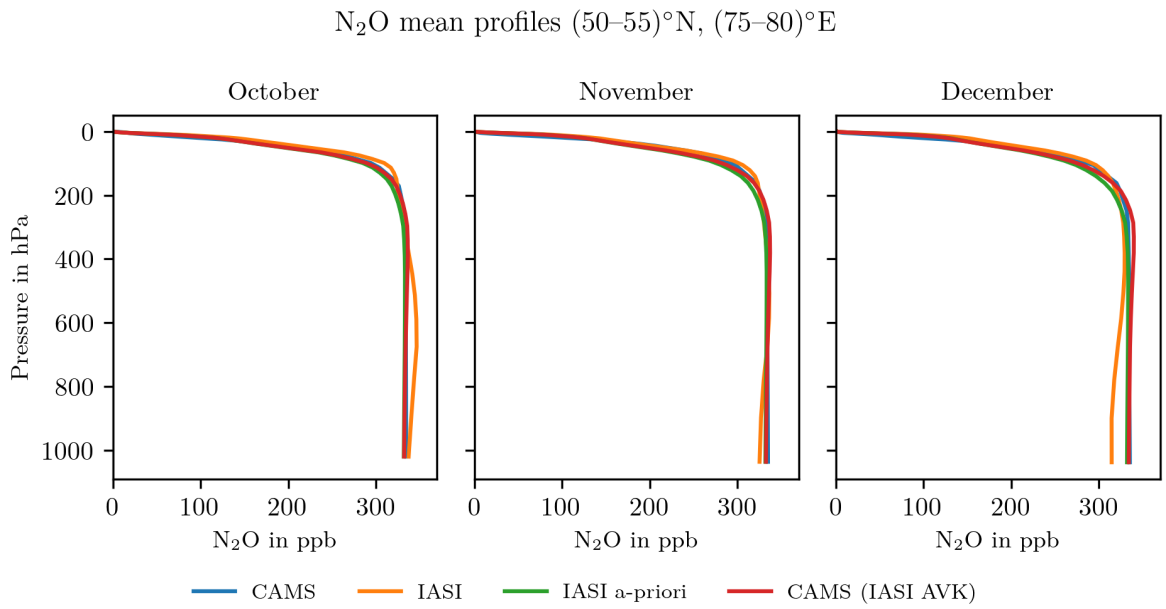

Figure 10: As **Figure 9** but for a grid cell over Siberia for October, November and December.

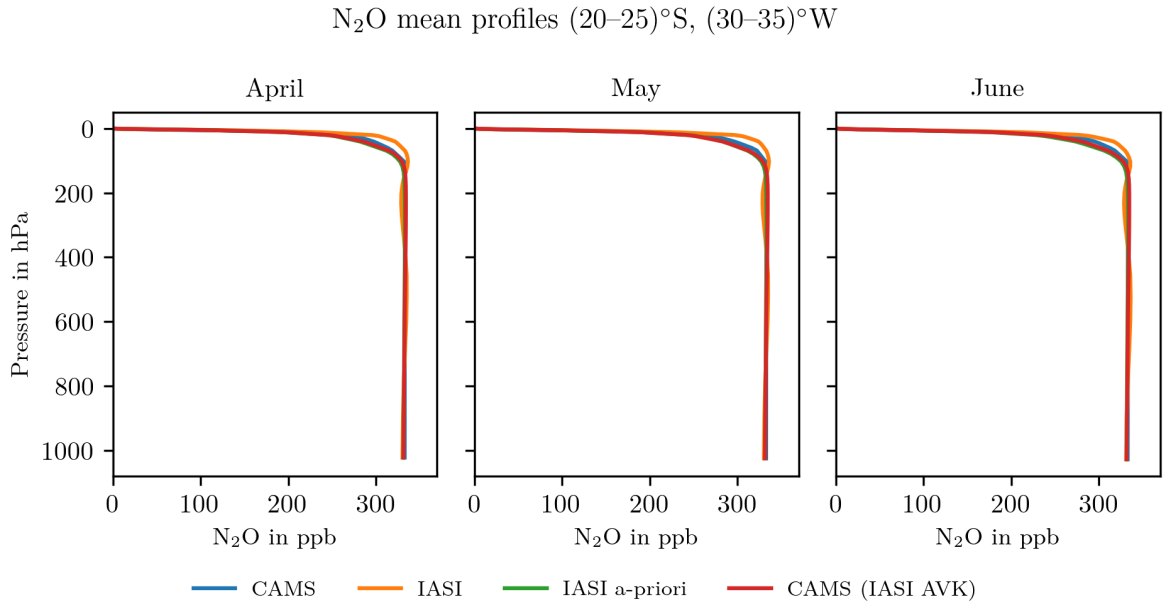

Figure 11: As **Figure 9** but for a grid cell over the Atlantic for April, May and June.

3.3 Zonal anomalies from IASI and CAMS

To remove the large-scale difference between the IASI and CAMS XN_2O data, we subtracted from each dataset its zonal mean value to obtain smaller scale variations given in each dataset. A prominent feature in the CAMS data are mountain ranges, which tend to show low values, as expected. In the IASI dataset, we observe much more variability and we also see low XN_2O value over the Himalayas and Greenland, but other mountain ranges such as the Rocky Mountains or the Andes show high values, which is not sensible. Also, other features seen in the anomaly maps for IASI cannot be explained, for example the high values in tropical Africa in March or the high values in southern Africa in September. The smaller-scale structures seem to rather be the result of retrieval issues rather than real features. Due to the modest latitude coverage of GOSAT-2, we have not repeated this for GOSAT-2.

This project has received funding from the European Union's Horizon Europe research and innovation programme under grant agreement No 101081395

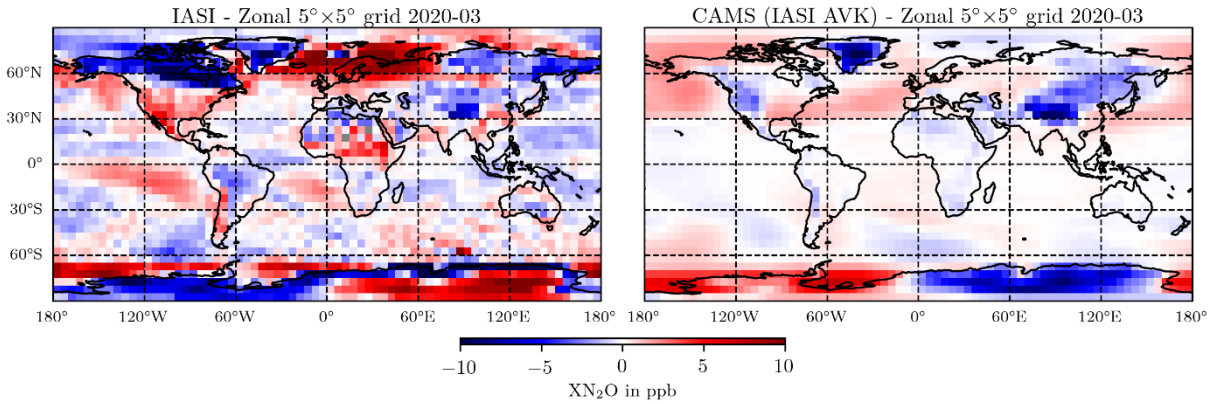

Figure 12: Zonal anomalies of XN2O from IASI and CAMS for March 2020

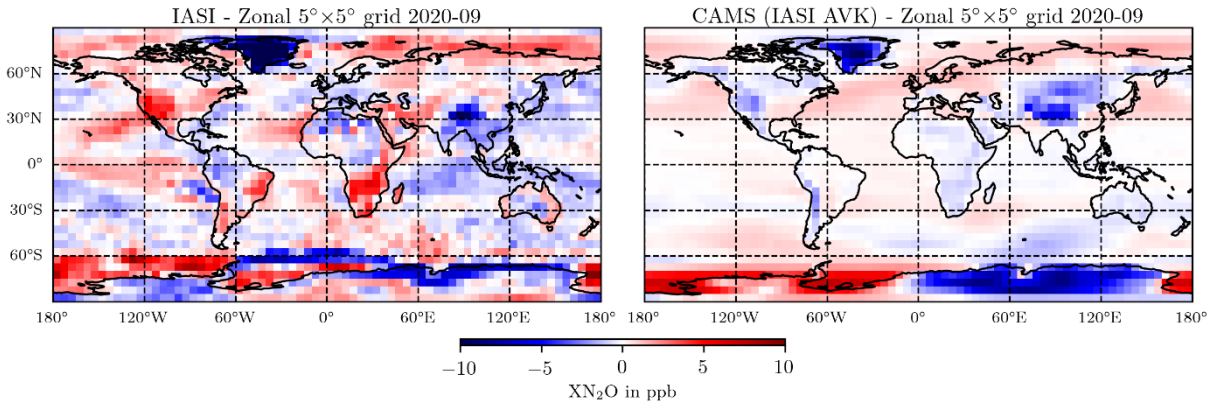

Figure 13: As **Figure 12** but for September 2020

3.4 Comparison between GOSAT-2 and IASI

Differences of XN_2O between IASI and GOSAT-2 are shown in Figure 14 and Figure 15. As already indicated in the comparisons of the satellite datasets to CAMS, we find that IASI XN_2O is typically higher than that from GOSAT-2 with a clear latitudinal trend. However, over some land surfaces, we find the opposite sign. The figures also give the zonal anomalies of the differences, which point towards clear negative values over bright desert surfaces and some land regions showing positive values. However, no clear picture emerges that would hint towards tropospheric emission patterns.

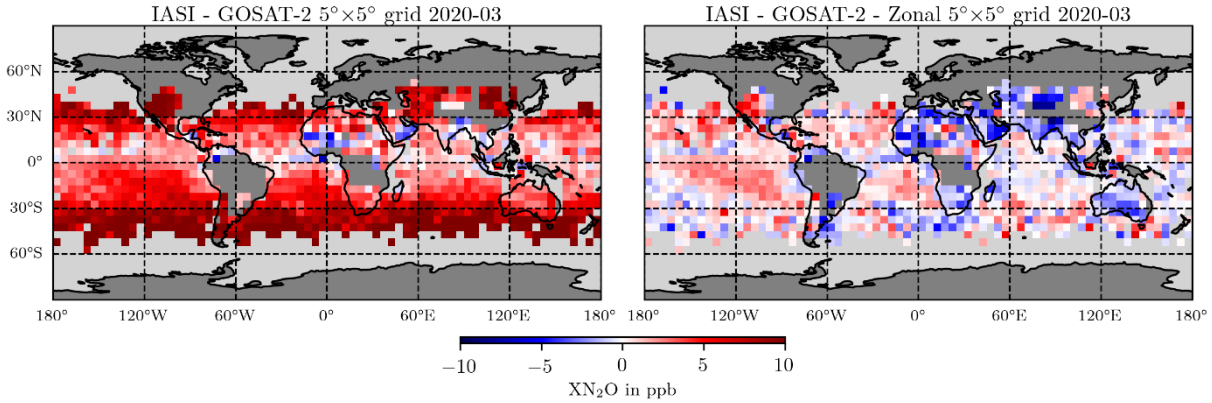

Figure 14: Difference between IASI and GOSAT-2 XN2O for March 2020 (left) and after removing the zonal average difference (right)

This project has received funding from the European Union's Horizon Europe research and innovation programme under grant agreement No 101081395

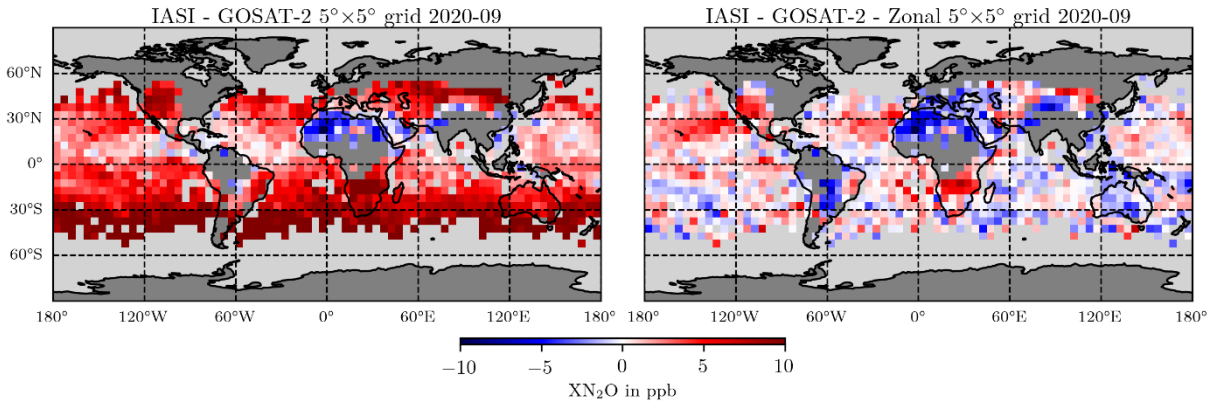

Figure 15: As **Figure 14** but for September 2020.

This project has received funding from the European Union's Horizon Europe research and innovation programme under grant agreement No 101081395

4. Conclusion and outlook

We have analysed XN_2O observations from the satellite instrument IASI and GOSAT-2 and contrasted them against CAMS model data. A key aspect of the two satellite datasets is their different vertical sensitivity with IASI measuring the free troposphere and stratosphere while GOSAT-2 measures the total column including the boundary layer. In principle, these different sensitivities could be used to remove the stratospheric column and to extract lower tropospheric N_2O values.

As expected, we observe a clear zonal structure in the satellite datasets and in CAMS data. However, the comparisons between CAMS and the satellite datasets reveal inconsistent results with higher XN_2O values in IASI and lower XN_2O values in GOSAT-2 compared to CAMS. For high latitudes, IASI also shows lower values. For GOSAT-2, the comparisons to CAMS are hampered by the low coverage, especially over land which is due to the strict quality filters that are applied.

In addition, we have: (1) evaluated zonal anomalies of XN_2O and of differences between satellites and CAMS to remove large scale differences, (2) compared selected vertical profiles and (3) directly compared IASI and GOSAT-2 XN_2O. The main conclusion is that observed features are more likely retrieval artifacts rather than real atmospheric features. Such artifacts are of the order of a few ppb which impede with any signals from surface emissions.

The main conclusion from this report is that satellite retrievals of XN_2O need to improve before they can be used with confidence to estimate emissions.

This project has received funding from the European Union's Horizon Europe research and innovation programme under grant agreement No 101081395

5. Acknowledgement

The figures shown in this report have been generated by Fabian G. Piwowarczyk and included in his Master thesis from the University of Bremen.

This project has received funding from the European Union's Horizon Europe research and innovation programme under grant agreement No 101081395

6. References

Anderson,G., S. Clough, F. Kneizys, J. Chetwynd, and E.Shettle. AFGL atmospheric constituent profiles (0–120km). Technical Report AFGL-TR-86-0110, Environmental Research Papers No.954, 1986.

Clerbaux, C., Boynard, A., Clarisse, L., George, M., Hadji-Lazaro, J., Herbin, H., Hurtmans, D., Pommier, M., Razavi, A., Turquety, S., Wespes, C., and Coheur, P.-F.: Monitoring of atmospheric composition using the thermal infrared IASI/MetOp sounder, Atmos. Chem. Phys., 9, 6041–6054, https://doi.org/10.5194/acp-9-6041-2009, 2009

Dutton, G. S., Hall, B. D., Dlugokencky, E. J., Lan, X., Nance, J. D., and Madronich, M.: Combined Atmospheric Nitrous Oxide Dry Air Mole Fractions from the NOAA GML Halocarbons Sampling Network, 1977–2023, Version: 2023-04-13, NOAA, https://doi.org/10.15138/GMZ7-2Q16, 2023.

Francey, R. J., Steele, L. P., Spencer, D. A., Langenfelds, R. L., Law, R. M., Krummel, P. B., Fraser, P. J., Etheridge, D. M., Derek, N., and Coram, S. A.: The CSIRO (Australia) measurement of greenhouse gases in the global atmosphere, Baseline Atmospheric Program Australia, edited by: Tindale, N. W., Derek, N., and Fraser, P. J., Bureau of Meteorology and CSIRO Atmospheric Research, Melbourne, 42–53, 2003.

Hourdin, F., Musat, I., Bony, S. *et al.* The LMDZ4 general circulation model: climate performance and sensitivity to parametrized physics with emphasis on tropical convection. *Clim Dyn* **27**, 787–813, https://doi.org/10.1007/s00382-006-0158-0, 2006

Marsh, D. R., M. J. Mills, D. E. Kinnison, J. Lamarque, N. Calvo, and L. M. Polvani, 2013: Climate Change from 1850 to 2005 Simulated in CESM1(WACCM). *J. Climate*, **26**, 7372–7391, https://doi.org/10.1175/JCLI-D-12-00558.1.

Noël, S., Reuter, M., Buchwitz, M., Borchardt, J., Hilker, M., Schneising, O., Bovensmann, H., Burrows, J. P., Di Noia, A., Parker, R. J., Suto, H., Yoshida, Y., Buschmann, M., Deutscher, N. M., Feist, D. G., Griffith, D. W. T., Hase, F., Kivi, R., Liu, C., Morino, I., Notholt, J., Oh, Y.-S., Ohyama, H., Petri, C., Pollard, D. F., Rettinger, M., Roehl, C., Rousogenous, C., Sha, M. K., Shiomi, K., Strong, K., Sussmann, R., Té, Y., Velazco, V. A., Vrekoussis, M., and Warneke, T.: Retrieval of greenhouse gases from GOSAT and GOSAT-2 using the FOCAL algorithm, Atmos. Meas. Tech., 15, 3401–3437, https://doi.org/10.5194/amt-15-3401-2022, 2022.

Prather, M. J., J. Hsu, N. M. DeLuca, C. H. Jackman, L. D. Oman, A. R. Douglass, E. L. Fleming, S. E. Strahan, S. D. Steenrod, O. A. Søvde, I. S. A. Isaksen, L. Froidevaux, and B. Funke, Measuring and modeling the lifetime of nitrous oxide including its variability. *J. Geophys. Res. Atmos.*, 120, 5693–5705. doi: 10.1002/2015JD023267, 2015

Prinn, R. G., Weiss, R. F., Arduini, J., Arnold, T., DeWitt, H. L., Fraser, P. J., Ganesan, A. L., Gasore, J., Harth, C. M., Hermansen, O., Kim, J., Krummel, P. B., Li, S., Loh, Z. M., Lunder, C. R., Maione, M., Manning, A. J., Miller, B. R., Mitrevski, B., Mühle, J., O'Doherty, S., Park, S., Reimann, S., Rigby, M., Saito, T., Salameh, P. K., Schmidt, R., Simmonds, P. G., Steele, L. P., Vollmer, M. K., Wang, R. H., Yao, B., Yokouchi, Y., Young, D., and Zhou, L.: History of chemically and radiatively important atmospheric gases from the Advanced Global Atmospheric Gases Experiment (AGAGE), Earth Syst. Sci. Data, 10, 985–1018, https://doi.org/10.5194/essd-10-985-2018, 2018.

Reuter, M.; Buchwitz, M.; Schneising, O.; Noël, S.; Rozanov, V.; Bovensmann, H.; Burrows, J.P. A Fast Atmospheric Trace Gas Retrieval for Hyperspectral Instruments Approximating Multiple Scattering—Part 1: Radiative Transfer and a Potential OCO-2 XCO_2 Retrieval Setup. *Remote Sens.*, *9*, 1159. https://doi.org/10.3390/rs9111159, 2017

This project has received funding from the European Union's Horizon Europe research and innovation programme under grant agreement No 101081395

Rodgers. C.D.R, I*nverse Methods for Atmospheric Sounding: Theory and Practice*. World Scientific, ,ISBN 9789812813718.doi:10.1142/3171, 2000

Schneider, M. and Hase, F.: Optimal estimation of tropospheric H_2O and δD with IASI/METOP, Atmos. Chem. Phys., 11, 11207–11220, https://doi.org/10.5194/acp-11-11207-2011, 2011.

Schneider, M., Ertl, B., Diekmann, C. J., Khosrawi, F., Weber, A., Hase, F., Höpfner, M., García, O. E., Sepúlveda, E., and Kinnison, D.: Design and description of the MUSICA IASI full retrieval product, Earth Syst. Sci. Data, 14, 709–742, https://doi.org/10.5194/essd-14-709-2022, 2022

Suto, H., Kataoka, F., Kikuchi, N., Knuteson, R. O., Butz, A., Haun, M., Buijs, H., Shiomi, K., Imai, H., and Kuze, A.: Thermal and near-infrared sensor for carbon observation Fourier transform spectrometer-2 (TANSO-FTS-2) on the Greenhouse gases Observing SATellite-2 (GOSAT-2) during its first year in orbit, Atmos. Meas. Tech., 14, 2013–2039, https://doi.org/10.5194/amt-14-2013-2021, 2021.

Thompson, R. L., Chevallier, F., Crotwell, A. M., Dutton, G., Langenfelds, R. L., Prinn, R. G., Weiss, R. F., Tohjima, Y., Nakazawa, T., Krummel, P. B., Steele, L. P., Fraser, P., O'Doherty, S., Ishijima, K., and Aoki, S.: Nitrous oxide emissions 1999 to 2009 from a global atmospheric inversion, Atmos. Chem. Phys., 14, 1801–1817, https://doi.org/10.5194/acp-14-1801-2014, 2014.

Tian, H., Pan, N., Thompson, R. L., Canadell, J. G., Suntharalingam, P., Regnier, P., Davidson, E. A., Prather, M., Ciais, P., Muntean, M., Pan, S., Winiwarter, W., Zaehle, S., Zhou, F., Jackson, R. B., Bange, H. W., Berthet, S., Bian, Z., Bianchi, D., Bouwman, A. F., Buitenhuis, E. T., Dutton, G., Hu, M., Ito, A., Jain, A. K., Jeltsch-Thömmes, A., Joos, F., Kou-Giesbrecht, S., Krummel, P. B., Lan, X., Landolfi, A., Lauerwald, R., Li, Y., Lu, C., Maavara, T., Manizza, M., Millet, D. B., Mühle, J., Patra, P. K., Peters, G. P., Qin, X., Raymond, P., Resplandy, L., Rosentreter, J. A., Shi, H., Sun, Q., Tonina, D., Tubiello, F. N., van der Werf, G. R., Vuichard, N., Wang, J., Wells, K. C., Western, L. M., Wilson, C., Yang, J., Yao, Y., You, Y., and Zhu, Q.: Global nitrous oxide budget (1980–2020), Earth Syst. Sci. Data, 16, 2543–2604, https://doi.org/10.5194/essd-16-2543-2024, 2024.

This project has received funding from the European Union's Horizon Europe research and innovation programme under grant agreement No 101081395

https://eyeclima.eu

BRUSSELS, 12 02 2026

Funded by the European Union. Views and opinions expressed are however those of the author(s) only and do not necessarily reflect those of the European Union. Neither the European Union nor the granting authority can be held responsible for them.

This project has received funding from the European Union's Horizon Europe research and innovation programme under grant agreement No 101081395